

LSPR-based colorimetric immunosensor for rapid and sensitive 17 β -estradiol detection in tap water

Antonio Minopoli^{a,b}, Nikola Sakač^c, Bohdan Lenyk^{b,d}, Raffaele Campanile^a, Dirk Mayer^b, Andreas Offenhäusser^b, Raffaele Velotta^a, Bartolomeo Della Ventura^{a,e,*}

^aDepartment of Physics “E. Pancini” – Università di Napoli Federico II – Via Cintia, 26 Ed. 6 – 80126 Napoli, Italy

^bInstitute of Complex Systems (ICS-8), Bioelectronics, Forschungszentrum Jülich, 52428 Jülich, Germany

^cFaculty of Geotechnical Engineering, University of Zagreb, Hallerova 7, 42000 Varaždin, Croatia

^dDepartment of Physics, University of Konstanz, 78457 Konstanz, Germany

^eDepartment of Physics, Politecnico di Milano, Piazza Leonardo da Vinci 32, 20133 – Milano (Italy)

*Corresponding author:
dellaventura@fisica.unina.it

Table of content

Figure S1. Functionalization study.

Figure S2. Characterization of naked and functionalized AuNPs.

Figure S3. Analysis of STEM image of a single AuNP.

Figure S4. Absorption spectra and DLS measurements at different E2 concentrations in tap water.

Figure S5. STEM images at low magnification acquired at different E2 concentration in tap water.

Figure S6. Analysis of STEM images of salt-induced aggregates of non-functionalized AuNPs.

Figure S7. Schematic representation of simulation workspace.

Figure S8. Simulated absorption spectra of 1-, 2- and 3-dimensional geometries.

Figure S9. Optical response of a linear chain with 3 AuNPs by varying the polarization angle.

Figure S10. Average simulated absorbance as a function of number of AuNPs along the linear chain.

Figure S11. Repeatability and stability assays.

Table S1. Schematic representation of 1-, 2- and 3-dimensional AuNP geometries.

Table S2. Electrical field distribution of 1- and 2-dimensional AuNP geometries.

Table S3. Data for the recovery assay.

Table S4. Example of serial dilution assay.

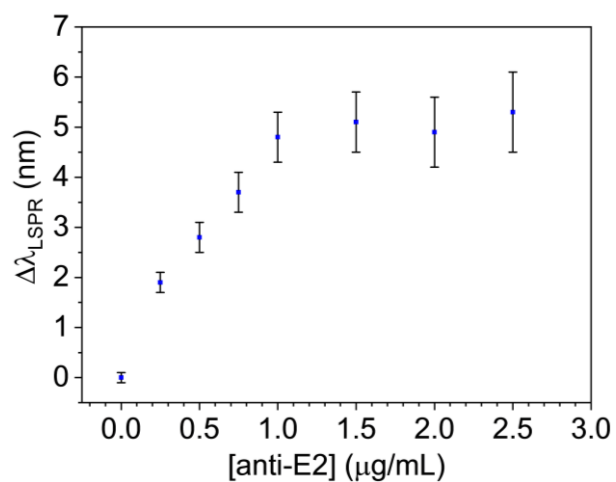


Figure S1. Functionalization study. Shift of the absorbance peak as a function of the anti-E2 concentration. The functionalization was achieved by adding 25 μL of irradiated Ab solution (18 $\mu\text{g/mL}$) to 1 mL of AuNPs (OD \sim 1.0). Such a volume was added in 5 spikes (5 μL each one) followed by gentle stirring to avoid AuNP aggregation. The absorbance peak red-shifted as the anti-E2 concentration increased until 1 $\mu\text{g/mL}$ that corresponded to a maximum red-shift of 5 nm. For larger amounts of anti-E2, all the AuNP surface was covered by anti-E2 and no change in LSPR wavelength was detectable.

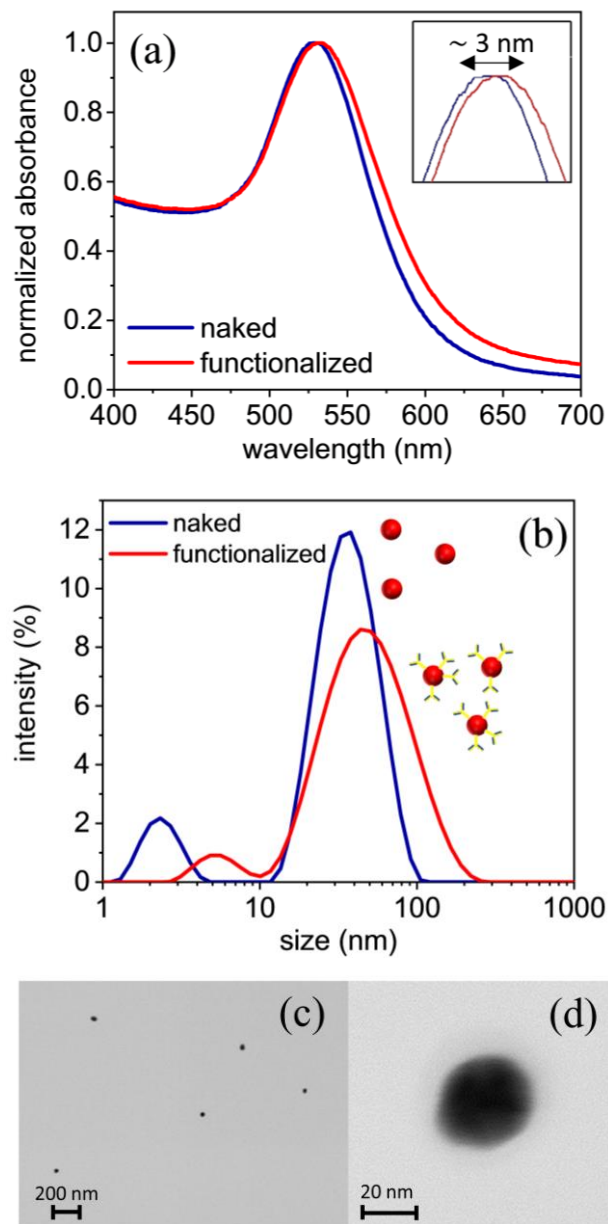


Figure S2. (a) Normalized absorption spectra and (b) DLS measurements of naked AuNPs (blue line) and functionalized AuNPs by anti-E2 (red line). STEM images of naked AuNPs at low (c) and high (d) magnification. The small red-shift of the absorbance peak (~ 3 nm) after the functionalization is due to the coverage of the AuNPs with a dielectric shell of thickness about 5 nm. The analysis of the STEM images (see also figure S3) highlights the presence of very regular spherical monodisperse nanoparticles with an average diameter of approximately 32 nm.

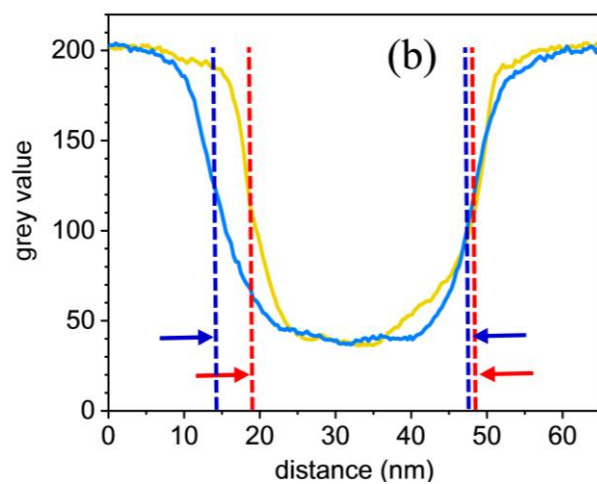
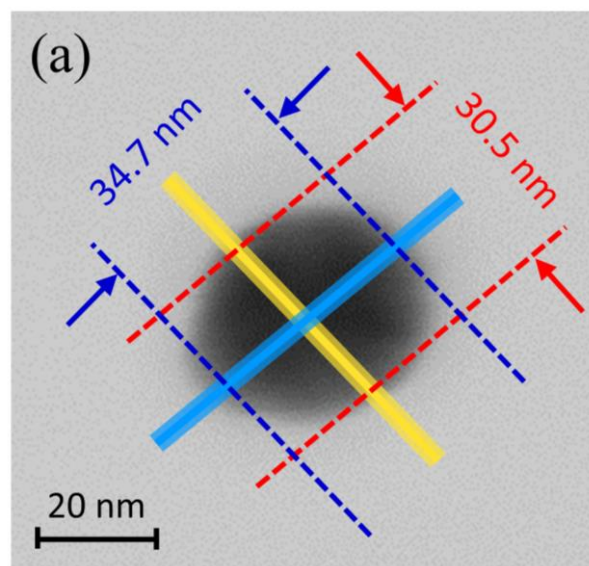


Figure S3. (a) STEM image of a single nanoparticle. The intensity profile measured along the yellow and blue line is reported in (b). The size measured as the FWHM of the intensity profiles confirms the synthesis of quite spherical AuNPs with an average diameter of approximately 32 nm.

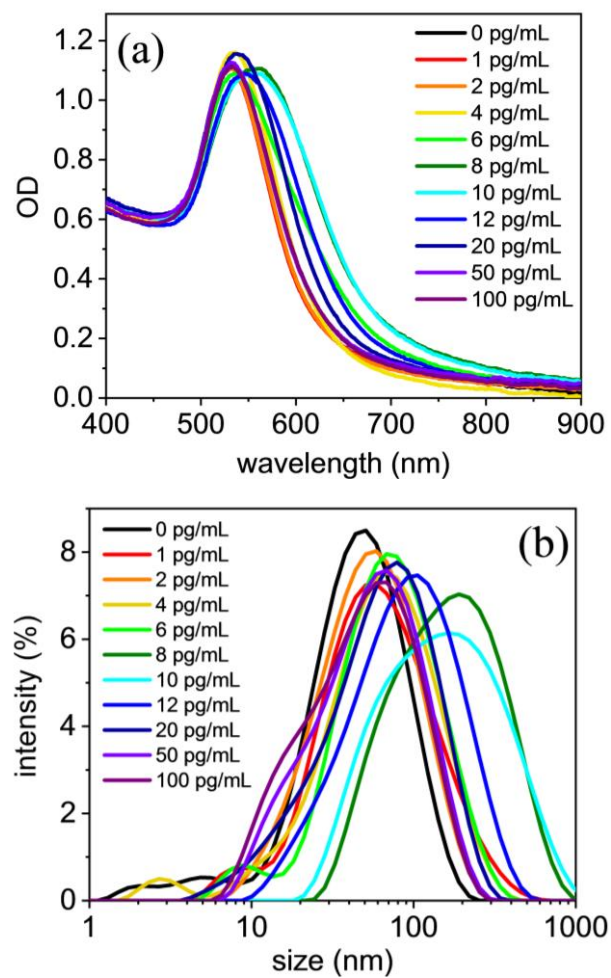


Figure S4. (a) Absorption spectra and (b) DLS measurements at all the E2 concentrations used in this experiment.

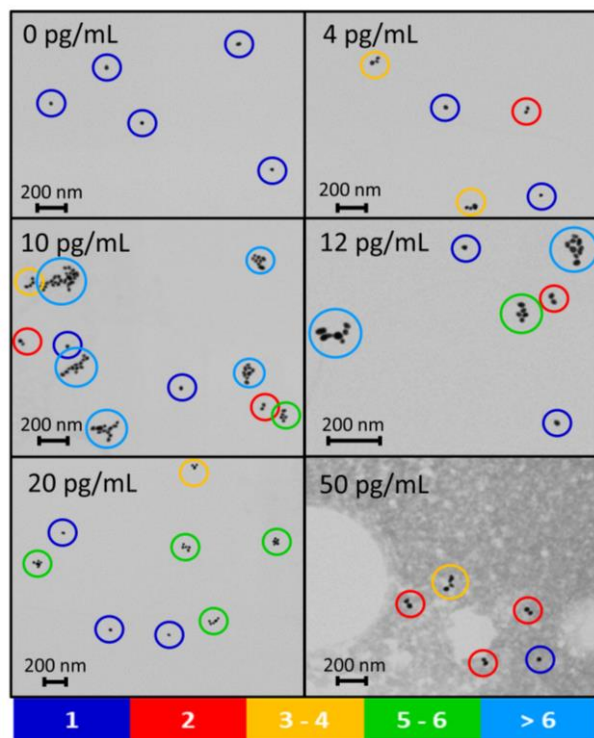


Figure S5. STEM images at low magnification acquired at different E2 concentration. The average number of AuNPs that form the aggregates approaches 12 AuNPs for the clusters corresponding to 10 pg/mL of E2. Further increase of the E2 concentration prevented AuNPs from forming larger clusters (*hook effect*). Nevertheless, the presence of dimers and trimers allowed us to achieve a measurable LSPR shift even at higher E2 concentration.

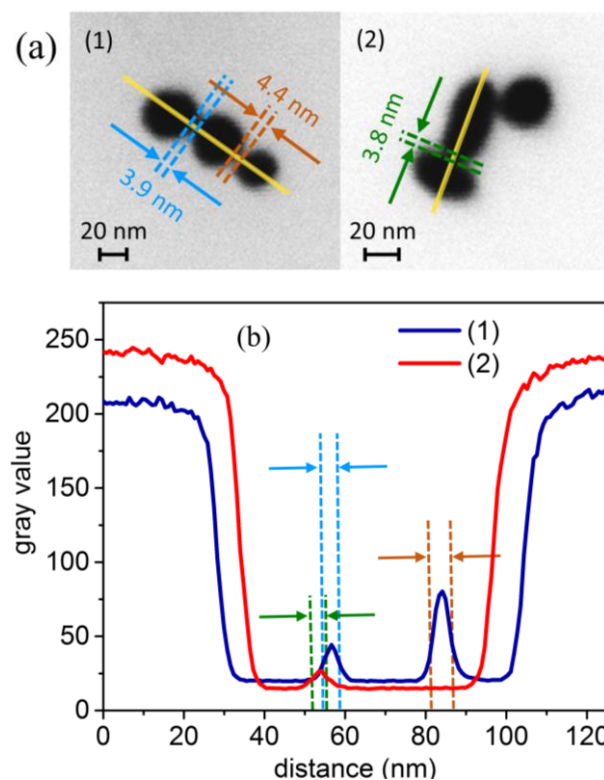


Figure S6. (a) STEM image of a salt-induced aggregate of non-functionalized AuNPs. The intensity profile measured along the yellow line is reported in (b). The interparticle distance measured as the FWHM of the cusps between adjacent nanoparticles is vanishingly small thereby confirming that no protein layer surrounded the AuNPs.

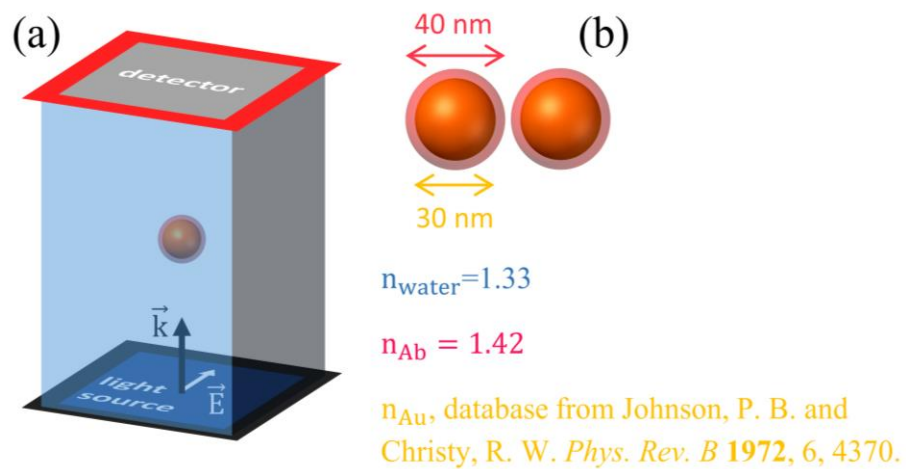


Figure S7. (a) Schematic representation of simulation workspace. (b) Geometrical parameters and refractive index of the materials. The optical response of the AuNP aggregates was simulated by the “FDTD solutions” tool of Lumerical.

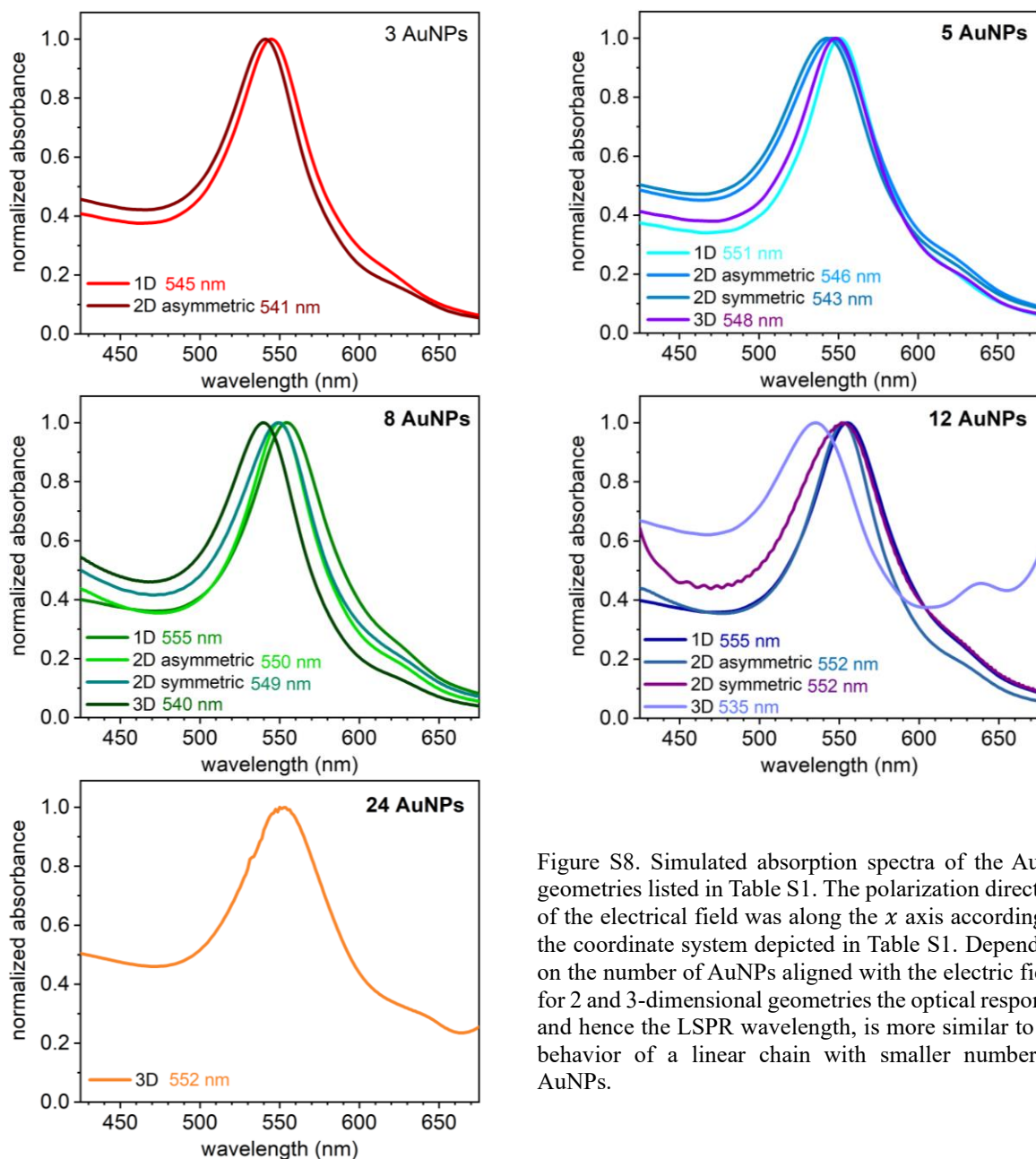


Figure S8. Simulated absorption spectra of the AuNP geometries listed in Table S1. The polarization direction of the electrical field was along the x axis according to the coordinate system depicted in Table S1. Depending on the number of AuNPs aligned with the electric field, for 2 and 3-dimensional geometries the optical response, and hence the LSPR wavelength, is more similar to the behavior of a linear chain with smaller number of AuNPs.

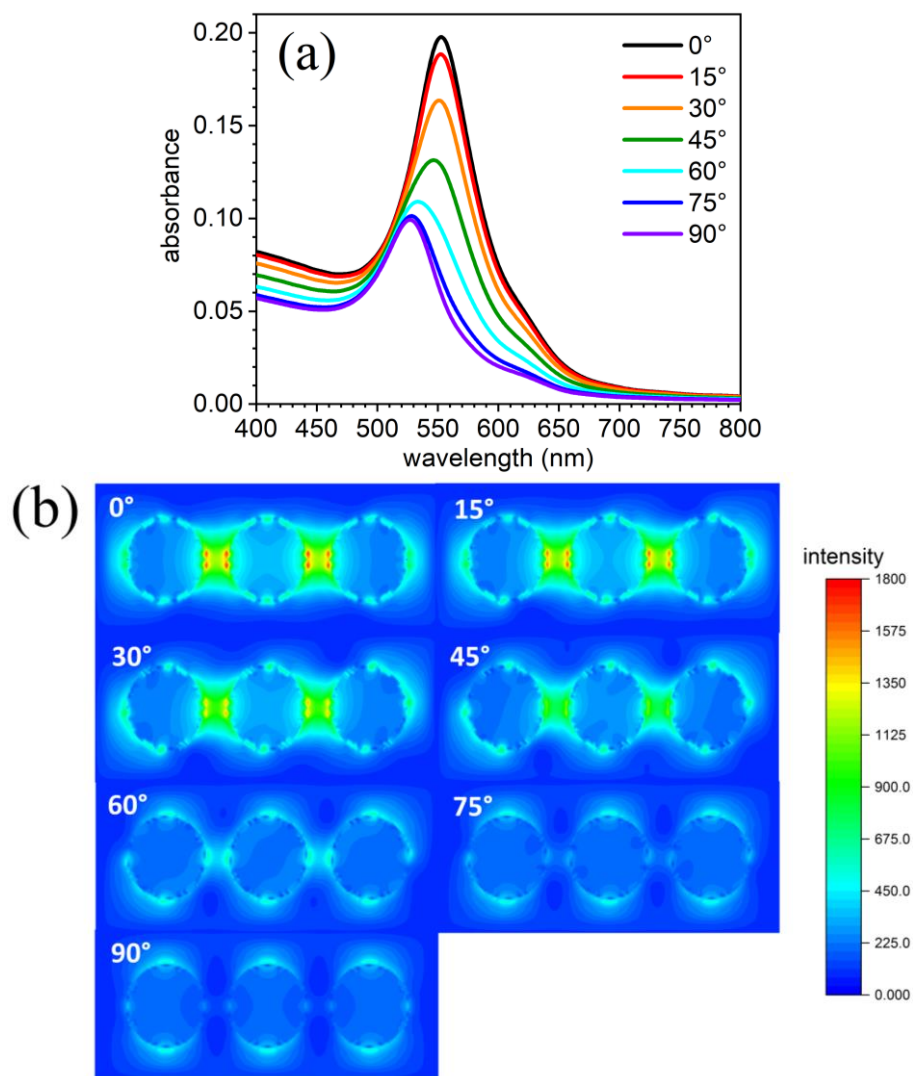


Figure S9. (a) Simulated absorption spectra and (b) electrical field distributions of a linear chain of 3 AuNPs as a function of polarization angle performed by “FDTD Solutions” tool of the software Lumerical. The absorption intensity and the LSPR wavelength decrease as the polarization angle increases moving from 0° (longitudinal mode) to 90° (transversal mode) due to a lower coupling among the AuNPs along the line.

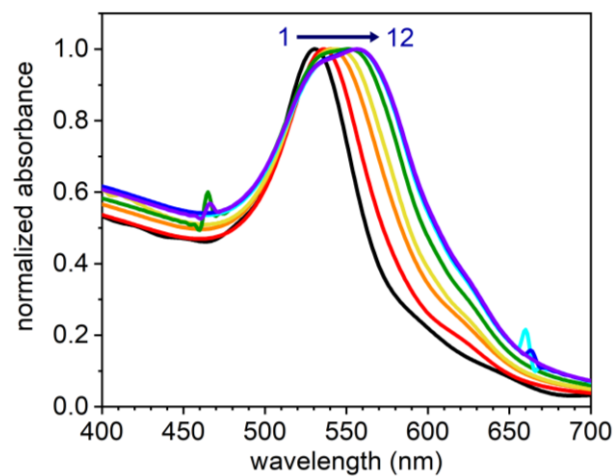


Figure S10. Average simulated absorbance of linear chains of AuNPs obtained by averaging the orientation of the chains with respect to the light polarization and by weighting for the angular distribution. Each spectrum $A(\lambda, \theta, N)$ was achieved by “FDTD Solutions” tool of the software Lumerical.

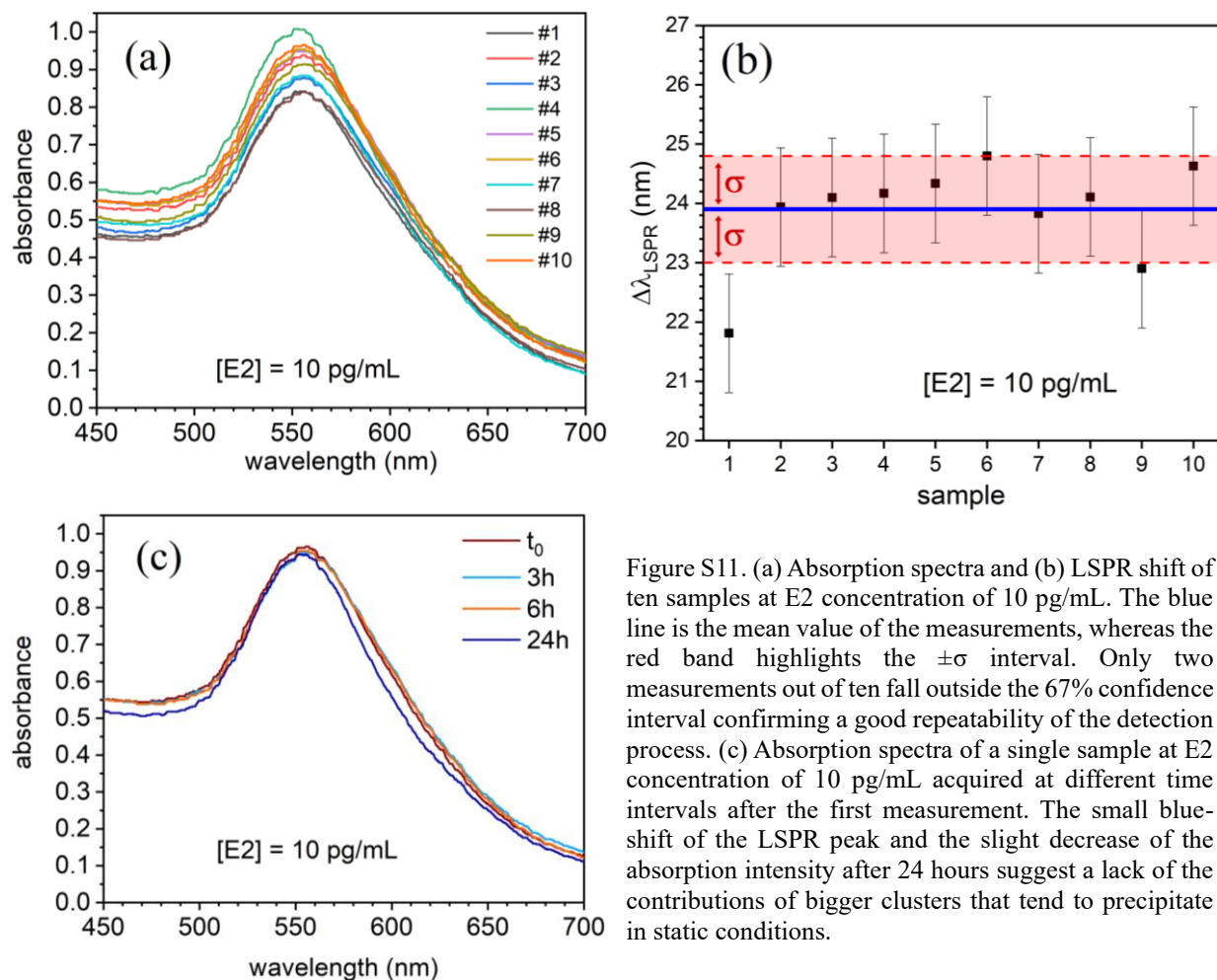


Figure S11. (a) Absorption spectra and (b) LSPR shift of ten samples at E2 concentration of 10 pg/mL. The blue line is the mean value of the measurements, whereas the red band highlights the $\pm\sigma$ interval. Only two measurements out of ten fall outside the 67% confidence interval confirming a good repeatability of the detection process. (c) Absorption spectra of a single sample at E2 concentration of 10 pg/mL acquired at different time intervals after the first measurement. The small blue-shift of the LSPR peak and the slight decrease of the absorption intensity after 24 hours suggest a lack of the contributions of bigger clusters that tend to precipitate in static conditions.

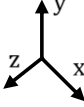
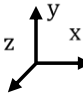
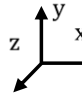
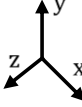




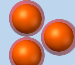
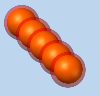
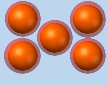
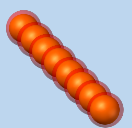
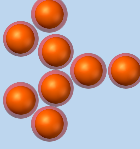
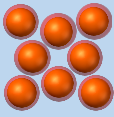
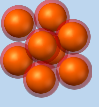
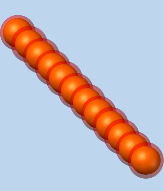
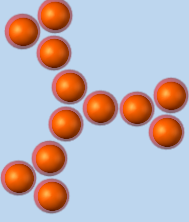
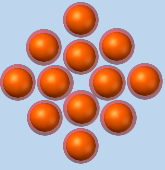

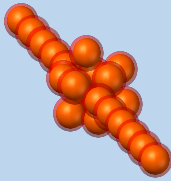
number of AuNPs	1D	2D asymmetric	2D symmetric	3D
				
1 (naked)				
1 (functionalized)				
2				
3				
5				
8				
12				
24				

Table S1. AuNP geometries taken into account for the optical simulations performed by “FDTD Solutions” tool of the software Lumerical. The distinction between asymmetrical and symmetrical 2-dimensional configurations refers to their possible symmetry with respect to the center of mass of the AuNP arrangement.

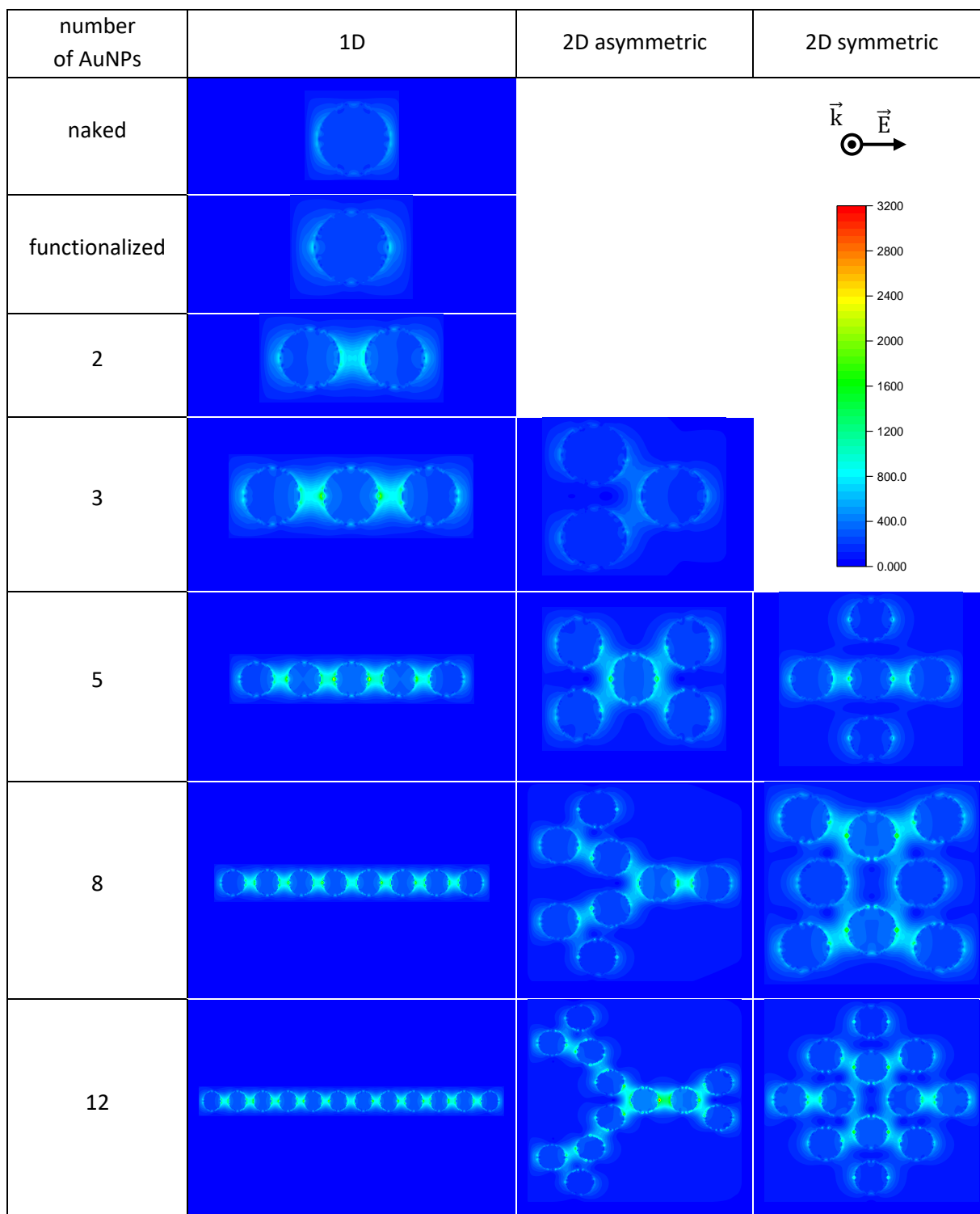


Table S2. Simulated electrical field distribution of 1- and 2-dimensional AuNP geometries listed in Table S1 performed by “FDTD Solutions” tool of the software Lumerical. The electrical field intensity was evaluated at LSPR wavelength of each configuration. The plasmonic behavior of more complex and branched geometries mainly arises from the AuNP lines aligned with the electrical field polarization.

nominal value	$\Delta\lambda_{\text{LSPR}}$	measured value	recovery
pg/mL	nm	pg/mL	%
4	3.6	4.9	122.5
6	7.1	5.4	90.0
12	17.3	15.1	125.8
20	9.1	18.5	92.5

Table S3. Data for the recovery assay.

[E2] pg/mL	dilution ratio				
	1:1	1:2	1:5	1:10	1:100
3	3	-	-	-	-
4	4	-	-	-	-
6	6	3	-	-	-
12	12	6	-	-	-
24	24	12	4.8	-	-
50	-	25	10	5	-
100	-	-	20	10	-
300	-	-	-	30	3
1000	-	-	-	-	10

Table S4. Example of a schematic approach to discriminate concentrations up to 1 ng/mL. The numbers in the cells represent the quantifiable E2 concentration with the corresponding dilution ratio. The concentrations out of the quantification range 3-30 pg/mL are omitted. By matching the LSPR shift of each sample dilutions with the values provided by the dose-response curve, it is possible to achieve an unequivocal response. The cells of interest were filled by analogous colors of the figure 2a in order to improve a visual reading of the table.